Tailor Made Concrete Structures – Walraven & Stoelhorst (eds)
© 2008 Taylor & Francis Group, London, ISBN 978-0-415-47535-8

Designing cast-in-situ FRC tunnel linings

B. Chiaia, A.P. Fantilli & P. Vallini
Politecnico di Torino, Torino, Italy

ABSTRACT: New procedures to design cast-in-situ steel fiber reinforced concrete (SFRC) tunnel linings are briefly presented in this paper. The ductile behavior at ultimate limit stage of such cement-based structures is ensured by a suitable amount of steel fibers and ordinary steel bars. The capability of SFRC to carry tensile stresses, also in the case of wide cracks, allows designers to reduce the minimum area of ordinary steel reinforcement, generally computed in compliance with American or European code requirements. In the serviceability stage, to evaluate crack widths more accurately, a suitable block model is introduced. This model is able to take into account the bridging effect of fibers, as well as the bond slip phenomenon between steel bars and SFRC in tension. Through the combinations of steel fibers and traditional reinforcing bars, it is possible to reduce the global amount of reinforcement in the structure, and contemporarily to increase the speed of construction. Consequently, the global cost of tunneling is reduced as well, particularly in massive structures. The proposed approach has been successfully applied to the design of two different tunnel linings in Italy.

1 INTRODUCTION

To obtain more durable and economic concrete structures, the combination of steel fibers and reinforcing bars represents a competitive design solution. In fiber reinforced concrete (FRC), the traditional rebars keep the main bearing function, but the global amount of steel can be significantly lower than in the case of classical reinforced concrete (RC). This is particularly true for lightly reinforced concrete structures subjected to bending and axial actions, like the massive structures of tunnel linings, where the combination of fibers and rebars (R/FRC structures) gives an increase of ductility, see Chiaia et al. (2007a).

In the case of beams in bending, due to the presence of fibers, tensile cracks are generally narrower and originate at small distances (Walraven 2007). As a consequence, the vulnerability of steel bars to corrosion is reduced and, contemporarily, the durability of concrete structures is increased. Therefore, the prediction of crack pattern, in terms of crack width w and crack distance s_r, is a fundamental point for the definition of the correct amount of steel reinforcement. Unfortunately, the evaluation of w and s_r in RC and R/FRC beams under bending and compression still remains an open problem. Despite the huge amount of investigations on RC structures in more than a century (for a review, see Borosnyoi & Balazs 2005), the existing formulae for evaluating crack width and crack spacing are not unanimously accepted. As a matter of fact, while the ACI 318-95 (1995) suggests an empirical approach for the evaluation of w (derived from the tests by Gergely & Lutz 1968), which is independent of crack distance, both CEB-FIP Model Code 90 (1993) and Eurocode 2 (2004) recommend the following semi-empirical formula:

$$w_k = s_{r,\max}(\varepsilon_{sm} - \varepsilon_{cm}) \tag{1}$$

where, w_k = characteristic value of crack width; ε_{sm} = mean strain in the reinforcement between the cracks; ε_{cm} = mean strain in the concrete between the cracks; and $s_{r,\max}$ = maximum crack spacing computed with:

$$s_{r,\max} = k_3\, c + k_1\, k_2\, k_4\, \frac{\Phi}{\rho} \tag{2}$$

where, k_1, k_2, k_3, k_4 = non dimensional coefficients (Eurocode 2 2004); Φ = bar diameter; and ρ = effective reinforcement ratio (the ratio between the area of reinforcement A_s and the effective concrete area in tension $A_{c,\mathrm{eff}}$).

This approach has been extended to R/FRC structures by the $\sigma - \varepsilon$ design method suggested by Rilem TC 162-TDF (2003). More precisely, according to some experimental results (Vandewalle 2000), the crack width of FRC beams with rebars is always predicted with Eq.(1), independently of the amount of steel fibers added to the concrete matrix. On the contrary, the fiber aspect ratio L/D (L = fiber length; D = fiber diameter) is taken into account in the formula for the evaluation of the maximum distance

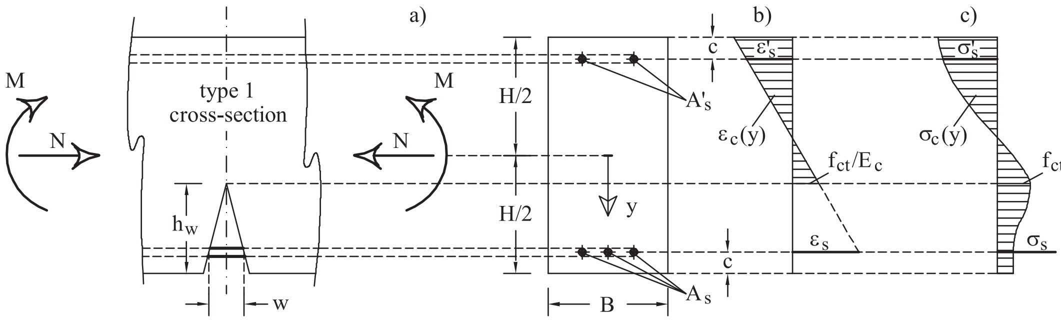

Figure 1. The cracked cross-section (type 1) subject to $M-N$: a) geometrical properties; b) strain profile; c) stress profile.

between cracks, which appears different from Eq.(2) (see Rilem TC 162-TDF 2003):

$$s_{r,\max} = \beta\, s_{r,m} = \beta\left(k_3 + k_1\, k_2\, k_4 \frac{\Phi}{\rho}\right)\frac{k_5}{L/D} \tag{3}$$

where, β = coefficient relating the average crack spacing to the design value; $s_{r,m}$ = average final crack spacing; and k_1, k_2, k_3, k_4, k_5 = non dimensional coefficients (Rilem TC 162-TDF 2003).

Eqs.(1–3) are not always effective for the prediction of real crack patters in RC and R/FRC members subjected to bending moment and normal forces. It is sufficient to recall that crack width is arbitrarily assumed to be in direct proportion with a unique value of crack distance, generally measured at stabilized crack pattern by Eqs.(2–3).

In a more realistic approach, w and s_r have to be computed contemporaneously by means of a block model like the one already introduced by Fantilli & Vallini (2004) for RC and R/FRC elements in tension. In this way, all the physical phenomena which affect the evolution of crack pattern (i.e. the bond-slip mechanism between steel and concrete and the nonlinear fracture mechanics of the cement-based material in tension) can be taken into account. Thus, the main target of this paper is to introduce an effective procedure for the prediction of crack pattern in RC and R/FRC members under combined bending and compression. In particular for the massive structures of tunnel linings, this model has to be used together with that already introduced by Chiaia et al. (2007a) for the evaluation of the minimum amount of steel rebars. In fact, according to Levi (1985), the criteria used to establish the minimum reinforcement percentages may regard both the ultimate limit state of the structure (i.e. the reinforcement must be dimensioned so that at the onset of cracking, the tensile stresses acting on the rebars will be prevented from exceeding its elastic limit) and the serviceability conditions (i.e. the local interaction between steel and concrete must keep the crack width within pre-established limits).

2 THE EVALUATION OF CRACK WIDTH IN RC AND R/FRC BEAMS

In RC and R/FRC beams, subjected to either constant or variable bending moments, it is practically impossible to predict a unique evolution of crack pattern (Fantilli et al. 1998). For these structures, due to the random nature of cracking, it appears more appropriate to define, for a given pair of applied actions $M-N$ (where, M = bending moment; and N = normal force), the maximum and the minimum values of crack width and crack spacing. This is possible by introducing a suitable block of FRC beam, in which w and s_r are computed by considering not only the bond-slip mechanisms between rebars and concrete in tension, but also the nonlinear behavior of cracked concrete under tensile actions. In this way, the states of stress and strain in the cracked cross-sections (called type 1) of the block can be defined. As shown in Figure 1, for given crack width w (measured at the level of reinforcement) and crack depth h_w (Fig. 1a), under the hypothesis of a linear strain profile between uncracked concrete and rebars in tension (Fig. 1b), strains in concrete $\varepsilon_c(y)$ and steel in tension ε_s and compression ε'_s [and the related stresses $\sigma_c(y)$, σ_s and σ'_s] can be obtained through the following equilibrium equations (Fig. 1c):

$$N = \int_{A_c} \sigma_c(y)\,dA + \sigma_s A_s + \sigma'_s A'_s \tag{4a}$$

$$M = \int_{A_c} \sigma_c(y)\; y\,dA + \sigma_s A_s\left(\frac{H}{2}-c\right) + \sigma'_s A'_s\left(\frac{H}{2}-c\right) \tag{4b}$$

where, y = vertical coordinate; c = concrete cover; A_c = area of concrete; A_s, A'_s = cross-sectional areas of steel rebars in tension and compression, respectively; H = height of the beam cross-section.

In a beam under bending and compression, the maximum crack width, corresponding to the applied loads M-N, is reached at incipient formation of new cracks (Fantilli & Vallini 2004), when also the crack distance

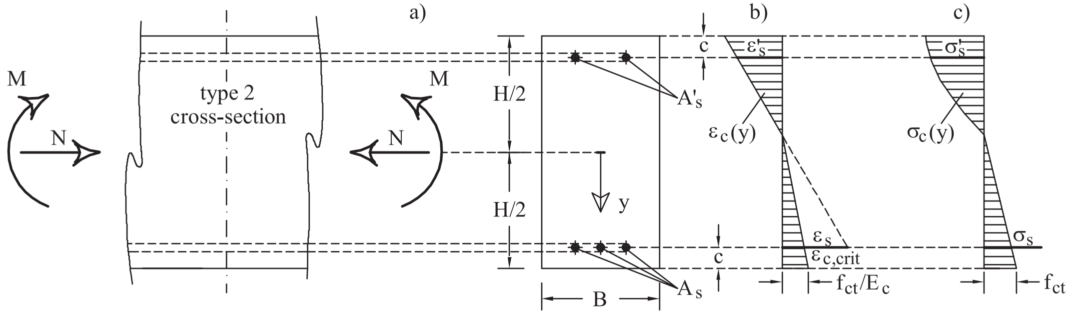

Figure 2. The cross-section at incipient cracking (type 2) subject to $M - N$: a) geometrical properties; b) strain profile; c) stress profile.

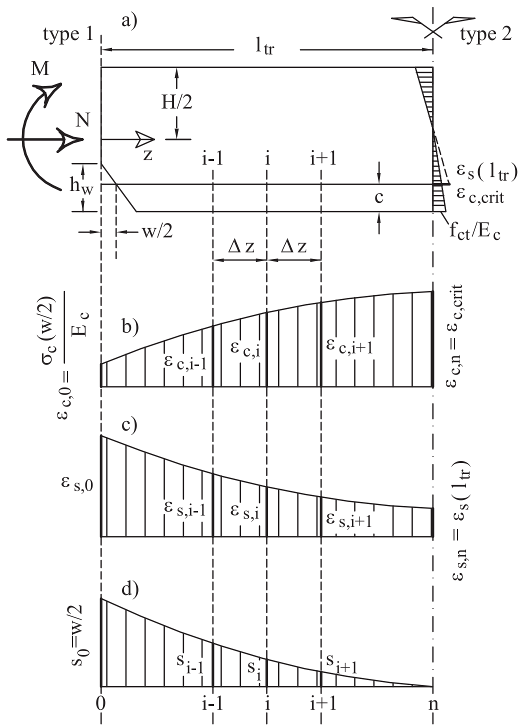

Figure 3. The block of the beam used for the evaluation of crack pattern.

is maximum. In general, due to the formation of a secondary crack pattern, the distance between primary cracks are halved and their widths are reduced (Clark 1956). The condition of incipient formation of a secondary crack is schematized in Figure 2a, where in a cross-section (called type 2) the tensile strength of concrete f_{ct} is reached at the lower edge in tension, while at the level of reinforcement, concrete reaches the critical strain $\varepsilon_{c,crit}$.

For the sake of simplicity, the strain profile is assumed to be bilinear: one slope for concrete in compression and steel bars in tension, whereas the other slope depicts concrete in tension (Fig. 2b). Also for type 2 cross-section, when $M - N$ are known, strains in concrete $\varepsilon_c(y)$ and steel (in tension ε_s and in compression ε'_s), as well as the related state of stress $\sigma_c(y)$, σ_s and σ'_s, can be obtained from Eqs.(4a-b) (Fig. 2c). The type 1 cross-section (cracked cross-section in Fig. 1) and type 2 cross-section (cross-section at incipient cracking in Fig. 2) limit the considered block (Fig. 3a), which reproduces the half beam's portion between two consecutive primary cracks at incipient formation of a secondary crack in between. Stresses and strains in the steel bars in tension, and in the surrounding concrete, can be calculated by the classical tension-stiffening equations:

$$\frac{d\sigma_s}{dz} = -\frac{p_s}{A_s} \cdot \tau \tag{5}$$

$$\frac{ds}{dz} = -\varepsilon_s(z) + \varepsilon_c(z) \tag{6}$$

where, p_s and A_s = respectively, the perimeter and the cross-sectional area of reinforcing bars in tension; s = value of slip between rebars and concrete; ε_s and ε_c = strains, respectively computed in the steel area in tension and in the tensile concrete at the same level of reinforcement ($y = H/2 - c$); z = horizontal coordinate; and τ = bond stress between steel and concrete.

If the constitutive relationship $\sigma - \varepsilon$ of the materials, the cohesive law $\sigma - w$, and the bond slip relationship $\tau - s$ are known, the complete analysis of the block can be performed. To be more precise, for given values of N and crack width w referred to the level of reinforcement, the relationship between crack width w and bending moment M can be obtained by solving Eqs.(4–6) with the following boundary conditions (Fig. 3a): $s(z = 0) = w/2$ (in the type 1 cross-section, where $z = 0$) and ε_c ($z = l_{tr}$) = $\varepsilon_{c,crit}$ (at level of reinforcement in type 2 cross-section, where $z = l_{tr}$). Due to the symmetry, in the type 2 cross-section $s = 0$ should be also verified.

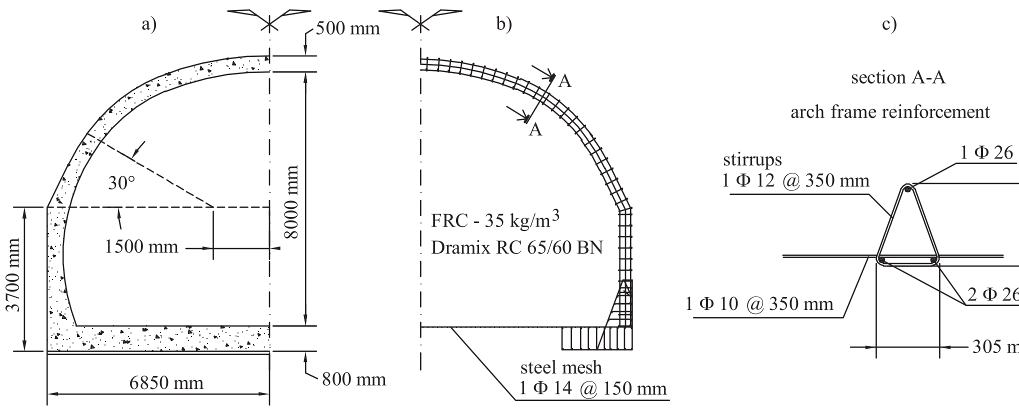

Figure 4. The cross-section FS27 of the Faver – S.S. 612 tunnel lining in Italy (Chiaia et al. 2007b): a) geometrical properties; b) steel bar arrangement in the whole cross-section; c) details of the arch frame reinforcement.

2.1 *Solution of the problem*

The model analytically described in the previous paragraphs can be numerically solved by the following iterative procedure (Fig. 3):

1. Assume a value for the normal force N.
2. Assume a value for the crack width w at level of reinforcement in the cracked cross-section (type 1) (Fig. 3a).
3. Assume a trial value for the crack depth h_w in the cracked cross-section (Fig. 3a).
4. From the equilibrium of type 1 cross-section [Eqs.(4a-b)] it is possible to obtain the applied bending moment M.
5. From the equilibrium of type 2 cross-section [Eqs.(4a-b)] it is possible to obtain the states of stress and strain in the cross-section at incipient cracking (in particular, it is possible to obtain the concrete strain at level of reinforcement $\varepsilon_{c,crit}$).
6. Assume a trial value for the length l_{tr} of the considered block, which is divided into n parts of length Δz.
7. Since the static and kinematical conditions are known at the borders of the considered block, it is possible to integrate numerically Eqs.(5–6) at the level of reinforcement. In a generic i-th point of the domain, the increments of concrete strains (Fig. 3b) are assumed to be similar to the decrements of steel strain (Fig. 3c), according to the following formulae:

$$\varepsilon_{s,i} = \varepsilon_{s,0} - \chi_i\left(\varepsilon_{s,0} - \varepsilon_{s,n}\right) \tag{7a}$$

$$\varepsilon_{c,i} = \varepsilon_{c,0} - \chi_i\left(\varepsilon_{c,0} - \varepsilon_{c,n}\right) \tag{7b}$$

where, $\varepsilon_{c,n}$ and $\varepsilon_{s,n}$ = strains in concrete and steel, respectively, in the type 2 cross-section; $\varepsilon_{c,0}$ and $\varepsilon_{s,0}$ = strains in concrete and steel, respectively, in the type 1 cross-section; and χ_i = coefficient of similarity ($0 \le \chi_i \le 1$). By applying the explicit finite difference method to Eq.(6), and by substituting Eqs.(7a-b), it is possible to define s_i as a function of χ_i:

$$s_i = s_{i-1} - \Delta z\left\lfloor \chi_i\left(\varepsilon_{s,n} - \varepsilon_{s,0} + \varepsilon_{c,0} - \varepsilon_{c,n}\right) + \varepsilon_{s,0} - \varepsilon_{c,0}\right\rfloor \tag{8}$$

where, $\Delta z = l_{tr}/n$ = length of the i-th part of the domain. Similarly, if the explicit finite difference method is applied to Eq.(5), it is possible to compute $\varepsilon_{s,i}$ according to the following equation:

$$\varepsilon_{s,i} = \varepsilon_{s,i-1} - \Delta z \frac{4}{E_s\,\Phi}\tau_{i-1} \tag{9}$$

In other words, the solution of the system of Eqs.(4–6) within the domain l_{tr} (which is a classical tension-stiffening problem for RC and R/FRC beams in bending) can be numerically obtained by moving from the point 0 to the point n and computing $\varepsilon_{s,i}$ with Eq.(9), χ_i with Eq.(7a), $\varepsilon_{c,i}$ with Eq.(7b) and s_i with Eq.(8).
8. If in the n-th point $s_n \neq 0$, change l_{tr} and go back to step 7.
9. If in the n-th point $\varepsilon_{c,n} \neq \varepsilon_{c,crit}$ (and therefore $\chi_i \neq 1$), change h_w and go back to step 4.

For a given couple of values N and w, the previous procedure gives the values of the bending moment M, and of the crack depth h_w in the cracked cross-section, the maximum crack width w_{max}, and the maximum distance between cracks $s_{r,max} = 2l_{tr}$ (the minimum distance between cracks is l_{tr}).

Such approach, in contrast with the semi-empirical requirements of the codes, permits to compute jointly all the main characteristics of the crack pattern. Moreover, with the increase of w and M, the experimentally detected reduction of l_{tr} is correctly predicted. On the contrary, some building codes impose a fixed value for the average distance between the cracks, which generally refers to the stabilized crack pattern at the end of the serviceability stage.

3 APPLICATION TO TUNNEL LININGS

The mechanical model previously described has been applied to the design of Faver – S.S. 612 tunnel lining in Italy (Chiaia et al. 2007b). In Figure 4a the geometrical properties of the cross-section FS27 are depicted.

The following points summarize the design process:

1. Starting from the geotechnical properties of the rock-mass, development of a finite element model to evaluate the actions during the excavation stages.
2. Definitions of bending and normal actions applied to the cross-sections of the tunnel lining.
3. Analysis, at ultimate limit states, of each cross-section; definition of the steel fiber volume, and, if necessary, evaluation of the minimum reinforcement area $A_{s,min}$ with the approach proposed by Chiaia et al. (2007a).
4. Analysis, at the serviceability limit stage, of each cross-section; evaluation of crack widths by means of the proposed model.

3.1 *M-N domains and the minimum amount of steel reinforcing bars*

Three design strength domains $M_{rd} - N_{rd}$ for a generic cross-section of the invert, are reported in Figure 5. One of them, referred to plain concrete, has been computed in accordance with the assumptions of Eurocode 2 (2003):

1. Plane sections remain plane.
2. The strain in bonded reinforcement, whether in tension or in compression, is the same as that in the surrounding concrete.
3. The tensile strength of the concrete is neglected.
4. The stresses in the concrete in compression are derived from the design stress/strain relationship (e.g., the parabola-rectangle diagram).

The $M_{rd} - N_{rd}$ domain for the SFRC and R/SFRC cross-section (reinforced by 35 kg/m^3 of Dramix RC 65/60 BN) has been obtained by adding the following hypotheses (Rilem TC 162-TDF 2003):

5. For steel fiber reinforced concrete, additionally reinforced with bars, the strain is limited to 25‰ at the position of the reinforcement.
6. Stresses in the steel fiber reinforced concrete are derived from the complete stress strain diagram.

In the case of Figure 5, the necessity of ordinary steel bars clearly appears, both for plain concrete and for SFRC cross-sections.

In fact, some of the points $M_{sd} - N_{sd}$ fall outside the computed strength domains $M_{rd} - N_{rd}$. The distance between the design actions and the border of these domains is not relevant (Fig. 5), thus a minimum amount of steel bars is necessary. The model proposed by Chiaia et al. (2007a) gives $A_{s,min} \cong 800\,\text{mm}^2$, both for the arch and the plane invert (Fig. 4). To be more precise, a steel mesh Φ14 mm@150 mm has been located in the top flange of the slab, while the self-sustaining steel truss depicted in Figure 4c represents the reinforcement in the arch.

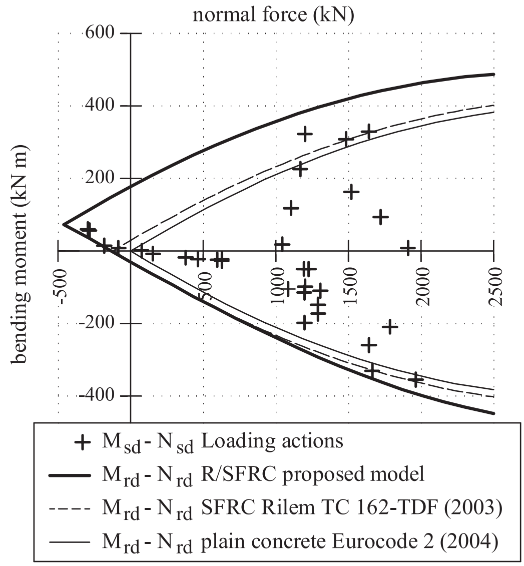

Figure 5. The compressive and bending actions $M_{sd} - N_{sd}$ compared to the design strength domains $M_{rd} - N_{sd}$ for the cross-section of the invert.

3.2 *Evaluation of crack width*

The calculation of the design crack width in R/FRC tunnel linings is similar to the case of a normal reinforced concrete structure. However, the tensile strength of steel fiber reinforced concrete after cracking has to be taken into account (Rilem TC 162-TDF 2003). The bridging action of fibers can reduce the crack widths normally observed in RC beams. This is clearly evident in Figure 6, where crack widths are computed for the invert under the quasi-permanent combination of loads, during the serviceability stage. In the same Figure, the results of three different approaches, obtained for classical concrete and FRC, are compared to those evaluated according to the proposed block model.

Under the same level of the applied actions (i.e. $N_{sd} \cong 0$ and $M_{sd} = 219$ kN m), the last model yields a value of crack width lower than 0.2 mm (which was the maximum allowed width). In other words, only with the block model here introduced, can the capability of steel fibers to reduce crack widths in R/FRC structures be effectively evaluated and successfully applied to design.

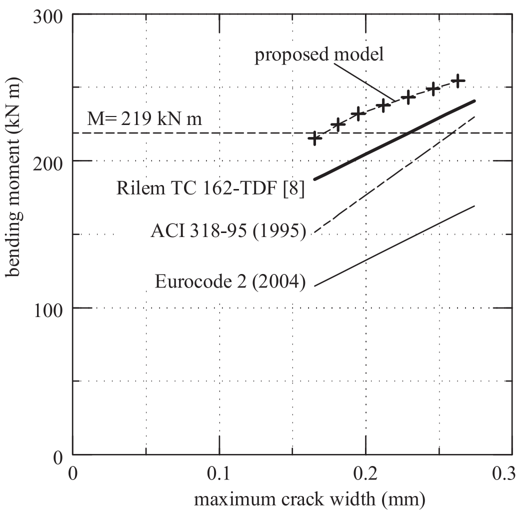

Figure 6. Crack widths in the invert of the FS27 cross section.

4 CONCLUSIONS

A new model, able to define crack width, crack spacing and crack depth in RC and R/FRC structures, has been proposed. From the comparison with the experimental data the following conclusions can be drawn:

- The proposed block model gives a more detailed evaluation of crack pattern. In particular, it provides the evolution of crack width, crack depth and crack distance with the increase of external actions, both in RC and R/FRC members subjected to bending and normal actions.
- The semi-empirical or empirical cross-sectional approaches, suggested by the code rules, do generally overestimate crack width, and thus underestimate the fiber contribution.
- The proposed model seems to confirm qualitatively the beneficial actions of the fibers in reducing the maximum crack width and crack distance, and thus in reducing the vulnerability of concrete structures to corrosion of the steel rebars.

The model here proposed for the analysis of crack patterns has to be used in conjunction with the model already introduced for the evaluation of the minimum reinforcement area of steel reinforcing bars (Chiaia et al. 2007a). In this way, it is possible to satisfy both the serviceability (SLE) and the ultimate (SLU) limit state conditions. In the case of cast-in-situ FRC tunnel linings, the presence of steel fibers provides relevant structural advantages with regard to both the limit states. Fibers reduce crack width and guarantee ductile failures, even in the presence of a low amount of steel bars. As a consequence, a faster advancement in construction, and a reduction of global costs, can be achieved. This has been successfully applied for designing the first cast-in-situ R/FRC tunnel linings in Italy.

ACKNOWLEDGEMNTS

The authors wish to express their gratitude to the Italian Ministry of University and Research for financing this research work (PRIN 2006), and to Bekaert for its continuous support.

REFERENCES

ACI 318-95 1995. Building Code Requirements for Structural Concrete. Farmington Hills, Michigan.

Borosnyoi, A., and Balazs, G. L. 2005. Models for flexural cracking in concrete: the state of art. Structural Concrete 6(2): 53–62.

Chiaia, B., Fantilli, A. P., and Vallini, P. 2007a. Evaluation of minimum reinforcement ratio in FRC members and application to tunnel linings. Materials and Structures 40(6): 593–604.

Chiaia B., Fantilli, A. P., and Vallini, P. 2007b. Minimum reinforcement and fiber contribution in tunnel linings: the Italian experience. In Xie Y M and Patnaikuni I (eds) ISEC 4. Proceedings of the Fourth International Structural Engineering and Construction Conference, Melbourne September 2007: 365–370.

Clark, A. P. 1956. Cracking in Reinforced Concrete Flexural Members. Journal of the American Concrete Institute, 27(8): 851–862.

Comitè Euro-International du Bèton 1993. CEB-FIP Model Code 1990. CEB Bulletin d'Information n. 213/214. Lausanne.

Fantilli, A. P., Ferretti, D., Iori, I., and Vallini, P. 1998. Flexural Deformability of Reinforced Concrete Beams. ASCE Journal of Structural Engineering 124(9): 1041–1049.

Fantilli, A. P. & Vallini, P. 200). Tension stiffening range in FRC elements. In di Prisco M et al. (eds) BEFIB 2004. 6th RILEM Symposium on Fibre Reinforced Concretes (FRC). Varenna September 2004: 847–856.

Gergely, P. and Lutz, L. A. 1968. Maximum Crack Width in Reinforced Concrete Flexural Members. In ACI-SP 20: Causes, mechanism and control of cracking in concrete, American Concrete Institute: 87–117.

ENV 1992-1-1 2004. Eurocode 2. Design of concrete structures – Part 1: General rules and rules for buildings.

Levi, F. 1985 On Minimum Reinforcement in Concrete Structures. ASCE Journal of Structural Engineering 111(12): 2791–2796.

Rilem TC 162 – TDF 2003. $\sigma - \varepsilon$ design method – final recommendation. Materials and Structures, 36: 560–567.

Vandewalle, L. 2000. Cracking behaviour of concrete beams reinforced with a combination of ordinary reinforcement and steel fibers. Materials and Structures 33: 164–170.

Walraven, J. C. 2007. Fracture mechanics of concrete and its role in explaining structural behaviour. In Carpinteri A et al. (eds) FRAMCOS 6. Fracture Mechanics of Concrete and Concrete Structures, Catania June 2007: 1265–1275.